Probabilistic mine design methods to reduce rockburst risk

by F.M.C.C. Vieira* and R.J. Durrheim†

Synopsis

There are many uncertainties that a mine designer should consider when selecting an optimal layout. Even though the inherent variability in the design parameters indicates that single-values are not representative of mining conditions, risk estimators such as ERR are often used without considering their statistical distributions. A probabilistic methodology has been developed to assess the influence of the *extraction sequence* and *layout geometry* on the rockburst risk associated with four ultra-deep mining layouts. The statistical distributions of incremental energy release rates and excess shear stresses at face elements are used as indirect estimators of rockburst risk in stopes, and the statistical distribution of the rock condition factor (RCF) is used as an indirect estimator of rockburst risk in tunnels and service excavations.

Introduction

Rock is a variable material, and it has long been recognized that rock failure is a continuous and complex structural breakdown process that should be regarded as stochastic (e.g. Hudson and Fairhurst[1969]) and that it is impossible to achieve the ideal of certainty in the design and operation of underground mines (Wane *et al.*[1964]). A value 200 MPa is often used for the uniaxial compressive strength (UCS) of quartzitic Witwatersrand rock masses, while the assumption that UCS is a *constant* is obviously a simplification (see Figure 1a). The *grade of the mineralization* (Figure 1b) and *stope-width* (Figure 1c) are other examples of variable mine design parameters.

A probabilistic methodology is used to assess the rockburst risk associated with four ultra-deep mining layouts that have different extraction sequences. We propose that the rock mass conditions during mining are better characterized by the statistical distribution of a characteristic variable than by a single average or median value. Probability theory and the related fields of statistics, decision and utility theory offer a framework for modelling uncertainty and evaluating the effects of certain variables on the overall mining scenario. This enables mine design decisions to be based on an objective and quantitative analysis of the trade-off between risk and benefit.

The methodology described here considers two aspects of mine design, viz. the extraction sequence and the layout geometry. A detailed description of the model orebody, mining methods and extraction sequence used in this study is given by Vieira *et al.*[2000] and is not repeated here, although the following characteristics should be noted:

- The longwall layout with strike pillars (LSP) advocates a breast advance sequence
- The sequential grid mining layout (SGM) advocates single-side breast mining in cyclic raise-availability periods. Pillars are orientated along the dip-direction
- The sequential down-dip mining (SDD) advocates down-dip extraction. Pillars are also orientated along the dip-direction
- Closely-spaced dip pillar mining (CSDP) also advocates down-dip extraction and has dip-orientated stability pillars.

Probabilistic rock engineering risk assessment

Risk

We have adopted the definition of Rowe[1977], who defines risk as *the potential for realization of unwanted, negative consequences of an event*. In the context of our evaluation, therefore, *events* refer to *damaging seismic events,* i.e. *rockbursts and unwanted consequences* mean (in hierarchical order) fatalities, accidental injury, property damage, resource loss, life-of-mine shortening, etc.

* *CSIR Miningtek, Auckland Park, South Africa.*

† *DEEPMINE, Auckland Park, South Africa.*

 SA ISSN 0038–223X/3.00 + 0.00. This paper was first presented at the SAIMM Symposium: Rockburst and Seismicity in Mines, *17–20 September 2001.*

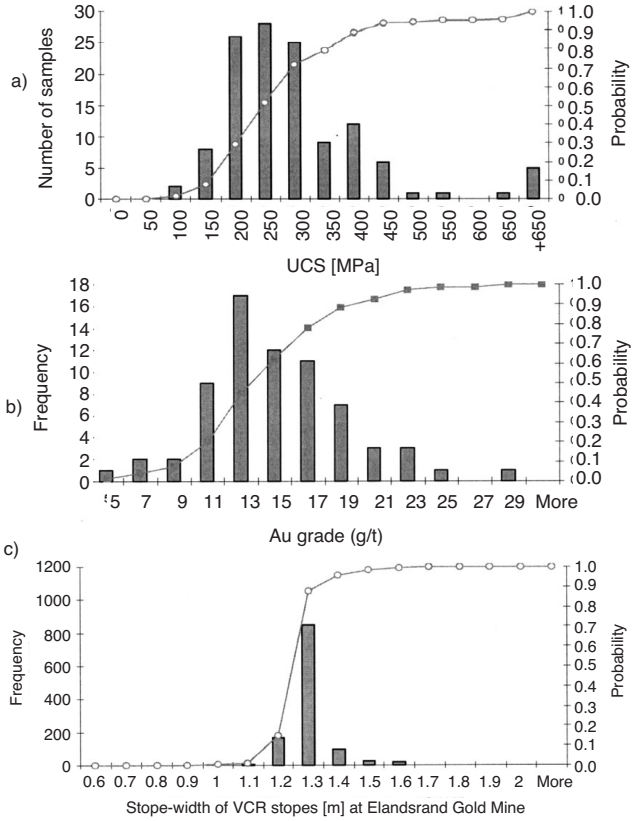

Figure 1—Variability of parameters used in mine design. (a) Variability of the UCS value of quartzitic rock on the Witwatersrand. UCS values are used in rock engineering support systems design. (b) Variability of grade in a typical Witwatersrand orebody (after Storrar[1981]). Grade is one of the most critical parameters in mine design and operations planning. (c) Variability of 'reported' stope-widths in sequential grid stopes, mining VCR

Risk is the combination of the likelihood or probability that an event will occur and the consequences if it does, i.e.

$$Risk = (Probability\ of\ an\ event) \times (Consequences\ of\ occurrence).$$

The consequence is affected by *exposure*, which depends on an individual's location with respect to *hazard areas*. The rockburst risk assessment procedures discussed here focus on those areas in the mine where, due to high levels of exposure, rockburst damage has the greatest unwanted consequences. These include areas in active on-reef faces, footwall tunnels and other ancillary excavations where large numbers of personnel are present. Situations where geological structures are especially vulnerable to seismic events (e.g. stopes approaching faults and dykes) are given special attention.

Risk estimators

Parameters that are widely used to assess the likelihood of a rockburst are listed in Table I. In this study we use the incremental energy release rate (ERR_i) between consecutive mining elements at each mining step; the maximum positive excess shear stress (ESS_{max}) along the plane of geological discontinuities in the vicinity of mining; the average pillar stresses (APS), and the rockwall condition factor (RCF) in footwall excavations beneath the regional stability pillars. In order to estimate the rockburst risk, we only consider those parts of the mine where people are likely to be present and exposed to the hazard. These parameters are determined by means of simulation using MINSIM 2000 (CSIR[2000]). Several new estimators have recently been proposed (e.g. Spottiswoode[1997,1999]; Van Aswegen *et al.*[2000]; Sanopoulos and Aswegen[2001]; Spottiswoode and Nxumalo[2001]), and could be used for a similar probabilistic analysis. The options open to the mine designer to reduce risk that were explored and evaluated include:

- Mining sequence
- Use of backfill
- Method of negotiating geological features, and
- Positioning of tunnels below pillars.

Risk acceptance levels

It is the responsibility of the operators of individual mines to define *the risk acceptance levels* or *thresholds* for their particular operations. Designs can then be accepted, modified or rejected when compared to the threshold. The threshold levels (x_a) of the risk estimators used here were set at workshops involving senior rock engineering practitioners working in deep-level gold mines: for ERR, x_a = 30 MJ/m^2; for ESS_{max}, x_a = 5 MPa; and for RCF, x_a = 1.

Risk estimation: basic principles

In general terms, if the continuous variable X is an *event* or *occurrence* that has a determinable probability, the *probability density function* (PDF) $f_X(x_i)$ of X, expresses the probability of the variable being associated with any one of its admissible values (e.g. the probability that ERR = 20 MJ/m^2). In the discrete case, it is termed the *probability mass function* (PMF). It is often necessary to know the probability that x exceeds a stated value, x_a (the risk acceptance level). For example, the probability that ERR will be below a threshold value, say P([Face ERR] < 30 MJ/m^2). More generally, the function $F_X(x_i)$ (see Figure 2), called the *cumulative distribution function* (CDF) of X, expresses the probability that a variable has a value less than or equal to a stated value of x. In the general case, therefore, if X is a discrete random variable with PMF $p_X(x_i)$, its CDF function is determined by

$$F_x(x) = P(X \le x) = \sum_{\forall x_i \le x} P(X = x_i) = \sum_{\forall x_i \le x} p_x(x_i) \quad [1]$$

The probability that a certain random variable X is in the interval (x, $x+\Delta x$) can be given by reading the values off its corresponding cumulative distribution function (CDF), as follows

$$P(x < X \le x = \Delta x) = F_x(x + \Delta x) - F_x(x) \quad [2]$$

Probability mass functions (PMF) were determined for all discrete random variables considered in this rock engineering assessment (ERRi, APS, ESS, RCF). The distributions were determined from data samples obtained from numerical modelling of scheduled mining scenarios derived from CADS mine models. Discrete cumulative distribution functions were subsequently derived from the PMFs.

Risk estimation: synthetic example

Consider the average pillar stress (APS) acting on a

Table I

Criteria for rock mechanics assessment of mine (adapted from Lightfoot and Maccelari[1999])

Criterion	Computation formulae	Application domain
Energy release rate	$ERR \approx 1/2 d_z \sigma_{zz}$	Seismicity related to regional layouts; Selection of support systems
Excess shear stress	$ESS = \lvert\sigma_s\rvert - (\sigma_n \tan \phi_0 + S_0)$	Bracket pillar design; Magnitude of shear-type events; Remedial measures (qualitative)
Average pillar stress	$APS = \frac{\sum_i S_{n_i}}{\sum_i a_i}$	Isolated pillar design; Stabilizing pillar design
Rock condition factor	$RCF = \frac{3\sigma_1 - \sigma_3}{F\sigma_c}$	Siting and support of service excavations
Off-reef principal stress	σ_{1i} (from MINSIM)	Siting and support of service excavations

where:

- dz vertical component of convergence at a rock mass element most recently mined
- σ_{zz} vertical stress component on a face element prior mining
- σ_s shear stresses acting on a discontinuity plane
- σ_n normal stress acting on a discontinuity plane
- σ_o contact friction angle of the discontinuity
- S_o initial contact cohesion of the discontinuity
- ϕ_o angle of internal friction
- S_n normal stress applied to elemental area a_i of a pillar (the overall area of the pillar being Σa_i)
- σ_1 major three-dimensional field stress components (major subsidiary principal stresses) acting normal to the long axis of a tunnel
- σ_3 minor three-dimensional field stress components (minor subsidiary principal stresses)
- σ_c uniaxial compressive strength of the rock, and
- F empirical rock mass condition factor (for competent rock $F = 1$)

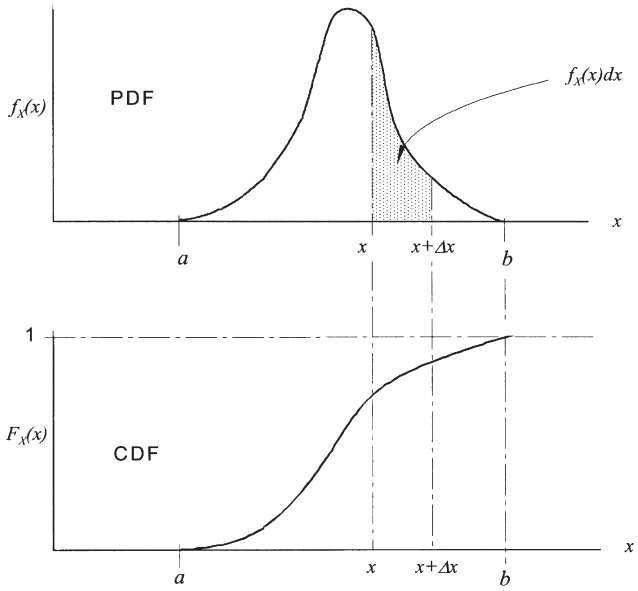

Figure 2—Graphical representations of the probability density function (PDF) and cumulative distribution function (CDF)

stabilizing pillar. APS is assumed to measure, indirectly, conditions of stability on a given pillar affected by adjacent mining activity. If, after comprehensive numerical modelling, one determines that the frequency diagram of all APS values on the pillar during a given period is as depicted in the histogram (Figure 3a), it is possible to determine the probability that pillar foundation failure will occur. If pillar foundation failure occurs when APS values are 600 MPa and greater (i.e. when these stresses exceed 2.5 times the UCS of the rock mass), the likelihood of pillar foundation failure is given by the probability that that APS will be equal or greater than 600 MPa, i.e. $P(APS \geq 600 \text{ MPa})$. The probability of this condition is accounted for by the dashed area in the PMF profile of the APS variable (Figure 3b), Alternatively, and more conveniently, one can use the correspondent cumulative distribution function (CDF) of APS (Figure 3c) to determine the risk of failure

$$P(600 > APS \leq +\infty) = F_x(+\infty) - F_x(600) \quad [3]$$

or, knowing that the probability of APS being less than 600 MPa is 0.84 (i.e. $F_{APS}(600) = 0.84$),

$$P(APS > 600) = 1 - F_x(600) = 1 \pm 0.84 = 0.16 \quad [4]$$

Thus there is a 16% chance that failure will occur, which is an indirect estimator of risk if we restrict our analysis to those parts of the mine where workers are exposed to the hazard.

Conditioning of risk estimators

In this risk assessment study, a simple technique was applied to filter out multiple counts of ERR at the same (x,y) position. The value of ERRi is given by the *increase* in ERR at face position (x,y) during mining step n, compared to the ERR at the same (x,y) position during a previous mining step, n-1. This is defined as follows:

$$ERRi(x,y)_n = ERR(x,y)_n - ERR(x,y)_{n-1} \quad [5]$$

It is important to recognize that, for a given mining step n, MINSIM computes point ERR values at face positions (x,y) as $ERR(x,y) \approx 1/2[\sigma_{zz}(x,y)n \times \sigma_{zz}(x,y)n]$, i.e. half the product of the vertical load (hangingwall stress σ_{zz}) on the solid element before it is mined and the convergence due to mining

(displacement S_{ZZ}) that occurs when the element is mined. Both the displacement and the stress at point (x,y) are influenced by the regional mining geometry. σ_{ZZ} is calculated

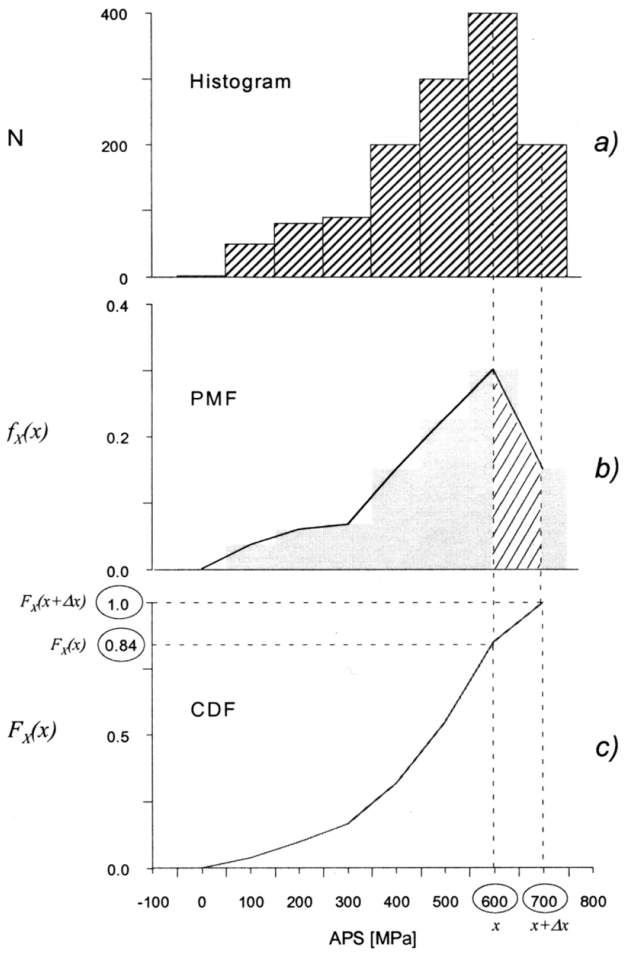

Figure 3—Average pillar stress (APS) distributions of a hypothetical deep stabilizing pillar

using the *stress intensity factor* that recognizes the loading influence of neighbouring elements. A consequence of the way ERR is calculated is that no energy is released unless the element (x,y) is mined and some convergence occurs. We know that even in the absence of active mining, some energy is released due to relaxation of the rock mass in back areas. The assumption that the rock mass in MINSIM is infinitely strong except in a small region near the active mining faces is thus a shortcoming of the current MINSIM ERR calculation scheme.

Figure 4 demonstrates the principle of incremental ERRs. A hypothetical mining sequence is represented, with faces advancing along the strike direction (x-direction) from step n=1 to n=m. Numbers inside each square polygon indicate the mining step during which the element area was mined. At mining step n=1 only three face elements are mined. Because this is the first step of mining, the incremental ERR ahead of active faces coincides with the nominal ERR, i.e. $\text{ERRi}(x,y)_n = \text{ERR}\ (x,y)_n$. At mining step n=2, face [1,1] did not advance further, in which case $\text{ERRi}(x,y)_n = 0$, since $\text{ERR}(x,y)n\ \text{ERR}(x,y)_{n-1} = 0$. At mining step n=3, a new face [1,4] started to be stoped and two others, faces [4,2] and [3,3] have advanced during this mining step. Ahead of these faces Equation [5] would be used in determining ERRi. Note that during step n=m, face [1,1] remains inactive. The result is that $\text{ERR}(x,y)_n$ is still the same as $\text{ERR}(x,y)_{n-1}$ for all preceding mining steps. The case of face [1,1], which advanced only once at step n=1, illustrates the usefulness of using ERRi rather than ERR for determining risk profiles. This element only contributed to the risk statistic during the period during which mining took place and personnel were exposed to the hazard of rockbursting.

Risk assessment methodology

The following procedure is used (see Figure 5).

Step 1: Define mining rules—Prior to conducting the risk assessment, the macro and micro design parameters such as

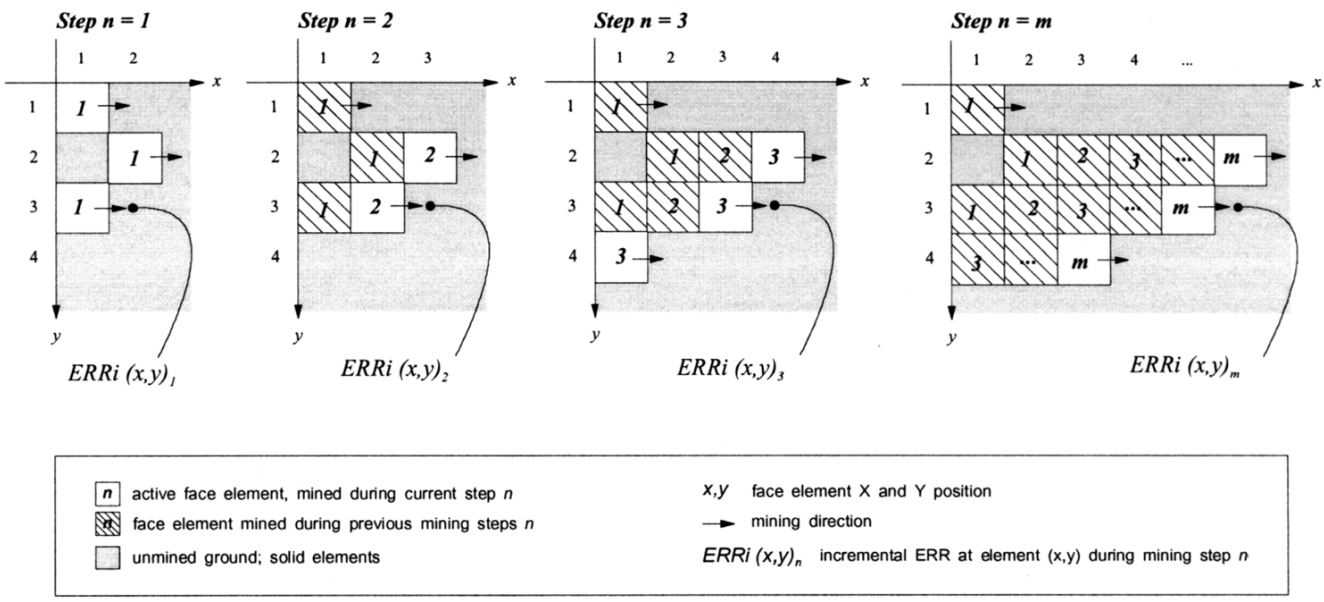

Figure 4—Concept of incremental ERR (ERRi) ahead of active mining faces. Polygons represent layout faces discretized as boundary elements in MINSIM

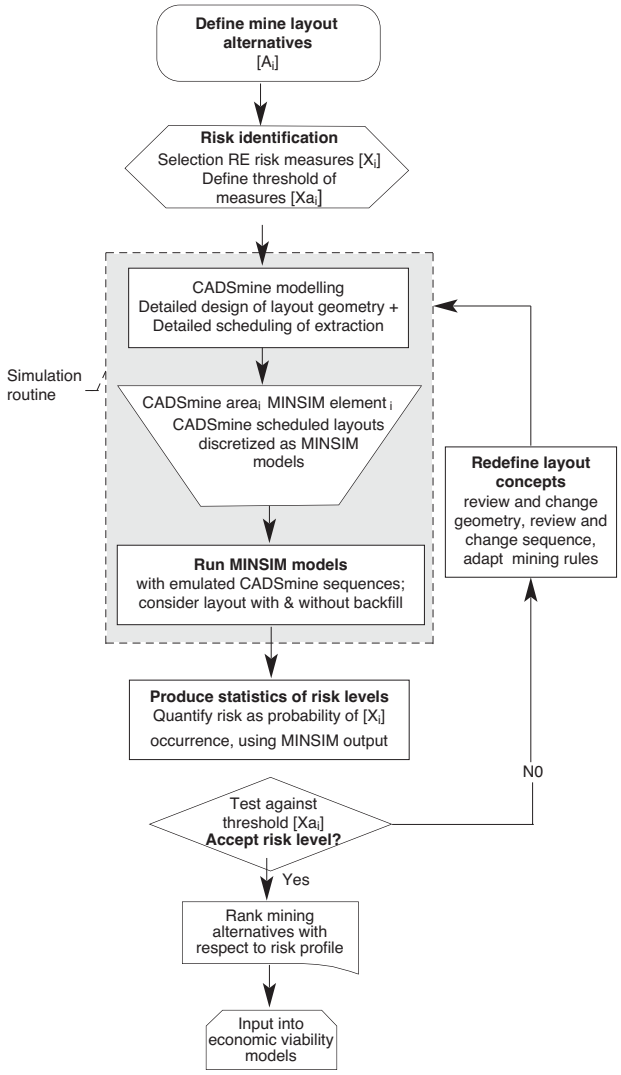

Figure 5—Applied methodologies for rock mechanics risk assessment of four mining alternatives

geometry (panel and pillar dimension, raise position, etc.) and extraction sequences are defined, as well as the constraints applied when mining near to geological structures (Vieira et al.2000).

Step 2: Select estimators of rockburst risk—The rockburst risk on the reef plane is estimated using ERRi (incremental energy release rate). Peak excess shear stress (ESS_{max}), the area of slip and the corresponding seismic moment are used when mining approached dykes and faults. The potential impact of seismicity on tunnels is inferred from the RCF.

Step 3: Simulate mining—The simulation routine requires *time of extraction* and the corresponding *area extracted* as inputs into MinSolve (CSIR2000) models, which are obtained from the CADSmine scheduling programme. An example of a life-of-mine CADSmine scheduled sequences is shown in Figure 6a, and the corresponding discretization into MINSIM is shown in Figure 6b. MINSIM models using the geometries of all four layouts were created, each within a solution space of 128×128=16,384 boundary elements with grid size of 14 m.

Step 4: Produce statistics of risk levels—A statistical treatment of the MINSIM output is used to derive probabilistic profiles of the risk measures for each mining layout. The determination of the risk measure is carried outside MinSolve, using a probabilistic treatment of the output variables such as that discussed above for the ERRi estimator.

Step 5: Compare with threshold—Results of the various rock related risk measures are then tested against pre-defined risk acceptance levels. Should the risk parameter be less than the threshold, the computation ends and the risk profile is stored for comparison with that from other layouts. Ultimately, the mining alternative are ranked with respect to the determined risk levels, after which a utility decision process is applied (Vieira1999).

Results

ERRi analysis

Stoping advances were scheduled in monthly intervals for the first five years of production, then quarterly up until the 12th year, and finally yearly until the end of the life of the mine. The 3-dimensional CADSmine model is considered a quasi-realistic representation of the topography of the reef surface,

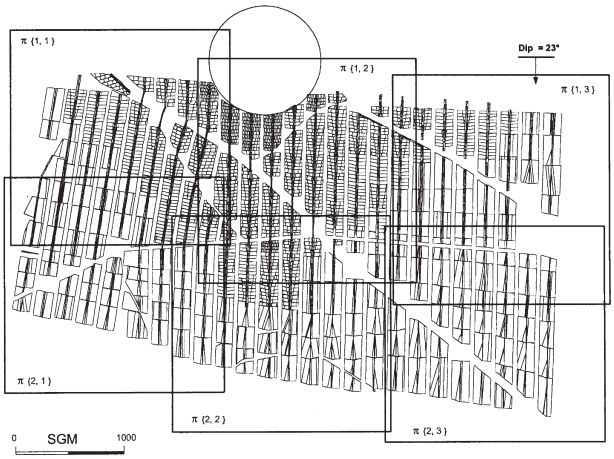

Figure 6a—CADSmine scheduling outlines for a sequential grid mine layout

Figure 6b—Boundary element discretization of the CADSmine model used for input into MINSIM

as it incorporates rolls and displacements on discontinuities. MINSIM discretization is a simplification, as the reef surface is assumed continuous and planar, dipping at 23° to the south. Only fault and dyke displacements on the reef plane are represented. The same input parameters and boundary conditions were applied to MINSIM models of all four mining layouts: a Young's Modulus of 70 GPa; Poisson's ratio of 0.2; depth dependent stress increment along of 0.0135 MPa/m for the horizontal components, and -0.027 MPa/m for the vertical component. Two operational scenarios were evaluated: no backfilling, and the introduction of backfill immediately after stoping. It was assumed that the fill material would react hyperbolically upon increasing loading, with a field stress reaction of up to 8 MPa for an ultimate compression of 0.45 m/m; and that the fill would have no cohesion with a friction angle of 30°. The fill width was considered 1.45 m, with an allowance of 0.05.m for shrinkage.

Figure 7 shows results from the assessment of the LSP layout. A frequency distribution and correspondent cumulative probability distribution of all ERRi occurrences during the scheduled life-of-mine of a LSP layout is shown. Similar calculations were made for other three layouts, resulting in the comparative risk profile charts in Figure 8a and Figure 8b. The benefits of applying backfill are observed by comparing the two charts. The risk rankings of these layouts for the two scenarios are listed in Table II, considering an ERRi threshold of 30 MJ/m^2. While there are quite large differences in the risk rankings among the various layouts, the effect of fill on any particular layout is small. Table II verifies that the SDD concept offers the best chance of low incremental ERRs ahead of active faces, for the modelling conditions considered. Taking the instance when no backfill is applied, SDD gives the highest probability of low face ERRi's, P(ERR<30 MJ/m^2) = 0.85. Note that the geometry of the SDD layout (75 m span with 25 m pillars) leads to the stiffest loading system of all and would, consequently, yield the lowest volumetric convergence and, hence, lowest ERR.

ESS analysis

Mining-induced seismicity may be divided into two classes: events associated with *crushing* of highly stressed volumes of rock, and events associated with *slip* or rupture along weakness planes in the rockmass. The likelihood of slip-type event occurring along pre-existing planes of weakness was estimated using the peak value of ESS and the area of ESS lobes (Ryder1988). Three dykes were studied. They were assumed flat and vertical, extending roughly 1000 m above and below the reef plane (see Figure 9).

To provide an indication of the relative increase of seismic hazard near discontinuities, positive ESS increments exceeding 5 MPa resulting from mining were considered (Figure 10). Most of the ESS distributions are bi-modal because of the regularly spaced pillars. High ESS values occurring in small areas may not trigger hazardous slip-type events, as it is the area of slip that controls the moment (and hence magnitude) of the mining-induced seismic event. The spatial distribution of ESS along the full length of the three dykes was evaluated (Figure 11). Modelling results show that the LSP layout develops the largest zones of positive ESS —positive ESS values greater than 15 MPa extended to areas

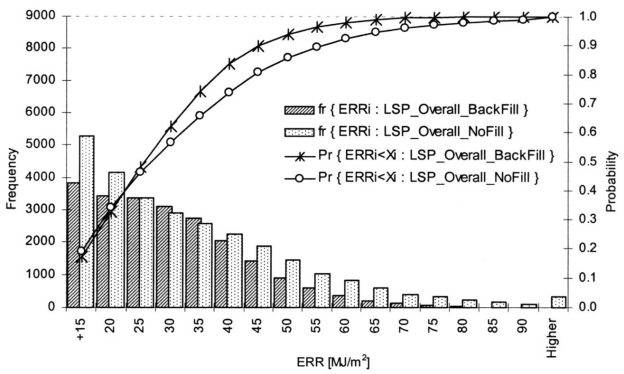

Figure 7—Overall ERRi frequency distributions and corresponding cumulative probability distribution for four ultra-deep mining layouts considering a mine-of-life sequence such as Figure 6a

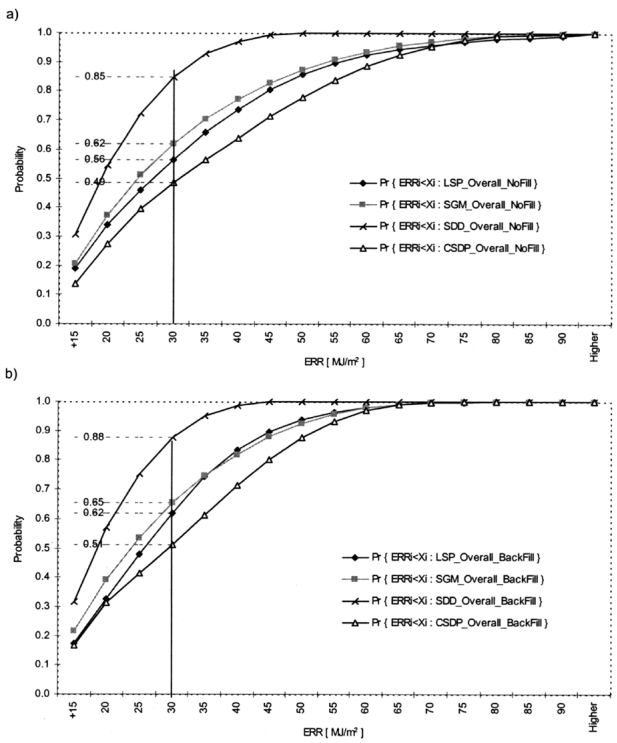

Figure 8—Risk profiles for four layouts using ERRi as risk estimator. (a) No backfill, (b) Backfill applied

Table II

Risk estimation with respect to the ERRi risk predictor for four layouts where stope extraction occurs with and without backfill

	No fill *P*(ERRi < 30 MJ/m^{-2})	Rank	Backfill *P*(ERRi < 30 MJ/m^{-2})	Rank	% benefit
LSP	0.56	3	0.62	3	6%
SGM	0.62	2	0.65	2	3%
SDD	0.85	1	0.88	1	3%
CSDP	0.49	4	0.51	4	2%

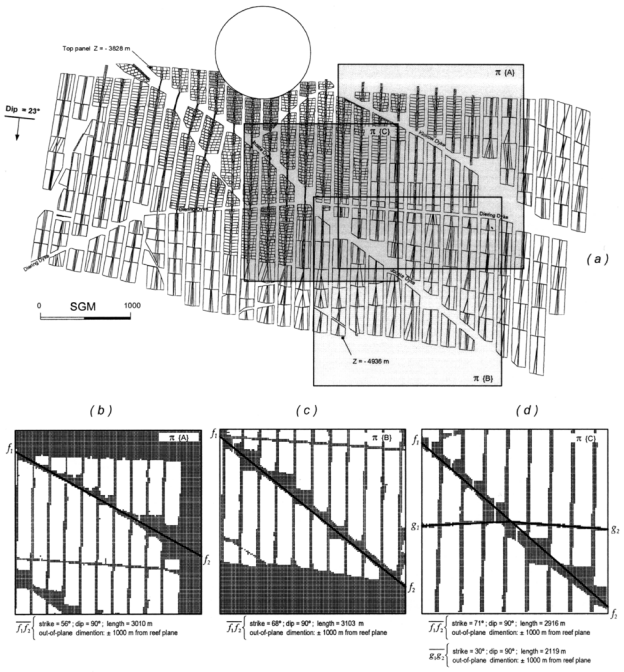

Figure 9—ESS models of macro layouts. (a) is the mine-wide reference domain; (b) the solution space π{A} to assess response near Klokow dyke (f_1f_2); (c) the solution space π{B} to assess response near Jooste dyke (f_1f_2); (d) the solution space π{C} to assess response of both Jooste (f_1f_2 and Diering dykes (g_1g_2)

as large as 200 m in length and 50 m wide (Figure 12a2). The effect of backfill in reducing the risk of slip-type events was investigated. The areas of positive ESS were determined using a digital planimeter. Results are shown in Table III, from which it can be inferred that stopes adjacent to geological features in an LSP layout benefit the most (26%) through the introduction of backfill. The SDD layout only benefits marginally, but was designed so that backfill would be unnecessary.

Examples of stepwise analysis results in partial domains for determining seismic parameters of interest, namely: *peak ESS, peak ride, seismic moment*, and retrieving *event magnitudes* of features are shown in the charts in Figure 13. The periods of advance considered coincided with yearly scheduled extraction periods. Because the period of advance is large, the seismic risk evaluations conducted here are rather crude. Global estimators of slip-type seismic risk for all modelled features in each layout are summarized in Table IV. The LSP layout has the highest risk for large slip-type events to occur, with magnitudes up to 4 being predicted, while the SDD layout appears to impart the best control of shear slip along discontinuities.

Multiple-attribute utility principles were used to rank the risks, following a scheme suggested by Vieira[1999] that uses a decision support tool called LDW (Smith[1998]). The hierarchy of risk measures in the risk assessment model is shown in Figure 14. The rock mass responses influencing the risk factor were measured in terms of the parameters listed in Table IV, now described as *risk measures*. In this example, equal weights were used for each dyke. Varied weights could be assigned, of course, to enforce desired *risk taker* profiles and to include possible trade-offs. The current assessment assumed no trade-offs resulting in a straightforward ranking. A matrix comprising the levels each risk measure is created with respect to each discontinuity, and each layout. Global weights are assigned to the various risk measures. A *utility* value is then determined for each variable, for each alternative. The utility values yield the ranking profiles in Figure 15. In the current ranking scheme, the highest level of utility denotes the lowest risk level for the layout, thus indicates the most preferred alternative. Conversely, the layout with the lowest utility is, thus, the layout presenting the highest overall seismic risk. The ranking profiles in

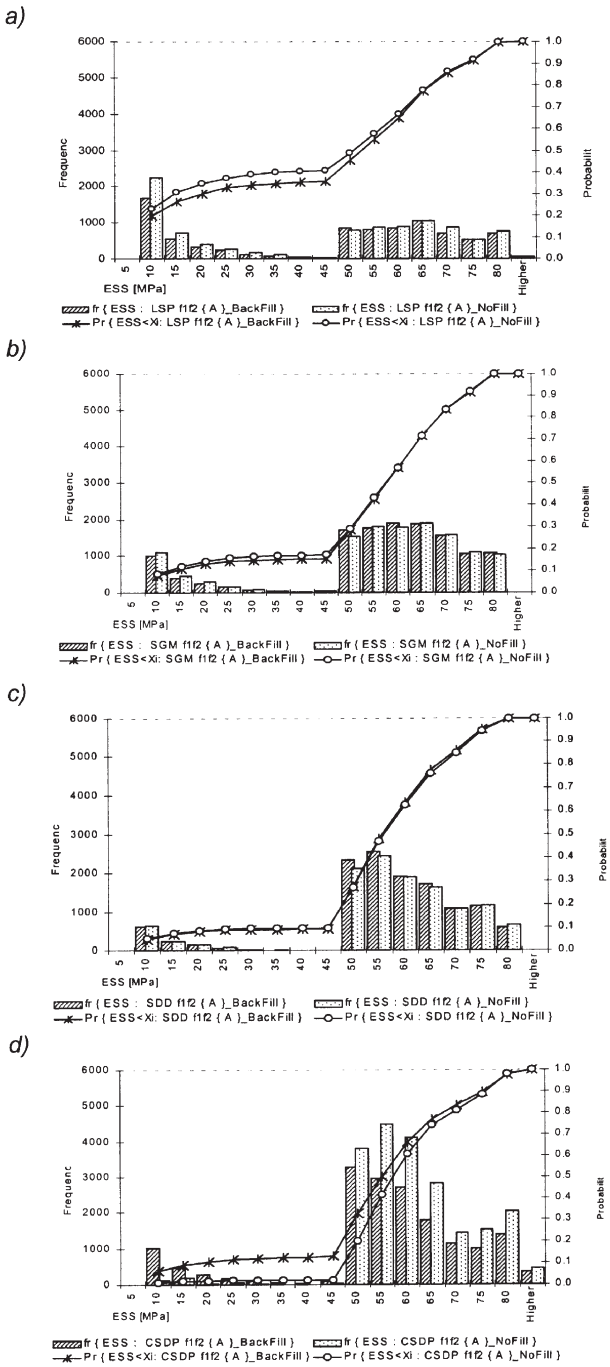

Figure 10—Distribution of positive increments of ESS for the four layouts over the life-of-mine along dyke plane in domain π{A} of Figure 9

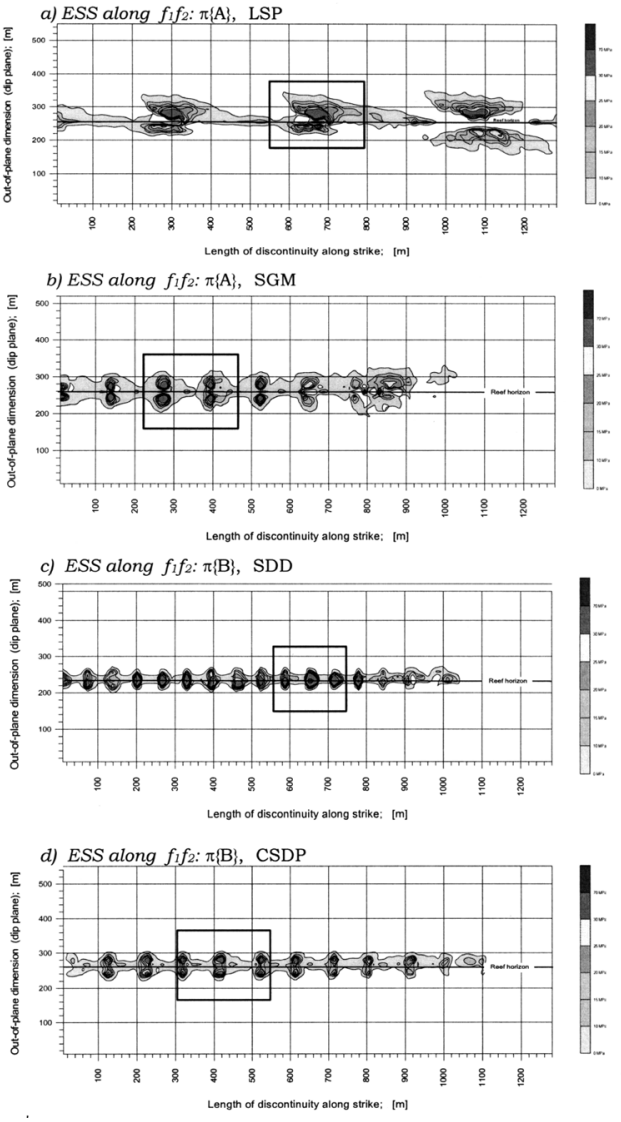

Figure 11—Limit stage ESS contours along geological features, when extraction in reef planes π{A} and π{B} is conducted by means of the LSP, SGM, SDD and CSDP sequence (backfill applied). Squared regions represent the areas where localized ESS effects were evaluated (see Figure 12)

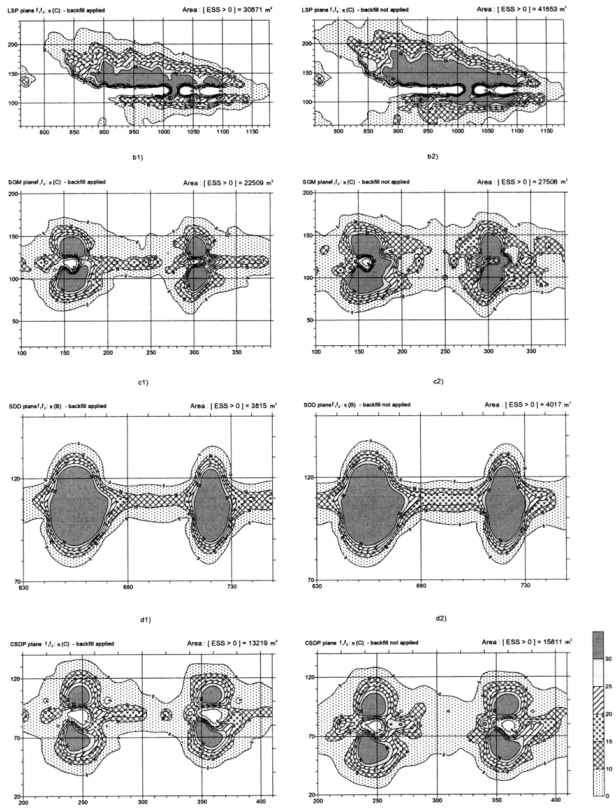

Figure 12—Localized ESS distributions on chosen slip-planes. The effect of backfill in reducing area of positive ESS is shown. All plots on the left refer to backfilled layouts; those on the right to non-backfilled layouts. Cross-lines in each plot coincide with a 50 m x 50 m reference eg. grid drawn on the plane of the feature

Table III

Area of positive ESS along representative dyke domains for backfilled and non-backfilled layouts

Layout	Feature	Area of ESS > 0		Backfill benefit
		Backfill [m²]	No fill [m²]	
LSP	f1f2: {C}	30871	41653	26%
SGM	f1f2: {C}	22509	27506	18%
SDD	f1f2: {B}	3815	4017	5%
CSDP	f1f2: {C}	13219	15811	16%

Figure 15a, drawn from the risk model in Figure 14, find that the SDD layout has the highest overall utility, thus the lowest seismic risk with respect to events generated by shear slip along discontinuities.

RCF analysis

A number of factors affect the stability of tunnels: the virgin stress, rock type and strength, shape and size of the excavation, the nature and design of support, the excavation method, and stress changes induced by nearby stoping. The extent of damage caused by seismically induced shaking is related to the condition of the tunnel walls. In this study, we made use of the rock condition factor (RCF) to estimate that effect of stoping on the stability of the main service tunnels (see Table I). If RCF<0.7, tunnel conditions are said to be excellent, if RCF>1 conditions rapidly deteriorate and increased levels of support resistance and areal coverage are required, and if RCF>1.4 severe deterioration of sidewall conditions is anticipated and a high degree of support is required).

If it is anticipated that conditions will be poor, it may be necessary to site the tunnels further below reef or, alternatively, modify the sequence of stoping. An iterative design process is often required, therefore, to arrive at an optimal layout design and scheduling that offers the lowest risk possible of tunnel instability, over its operational life. The numerical model input constraints applied were the same as for the on-reef assessment studies. Stoping was assumed to occur at an average depth of 4000 m below surface, and the entire pre-defined position of the various tunnels were monitored for stress changes as mining proceeded.

Access ways and return airways in LSP layouts are post-

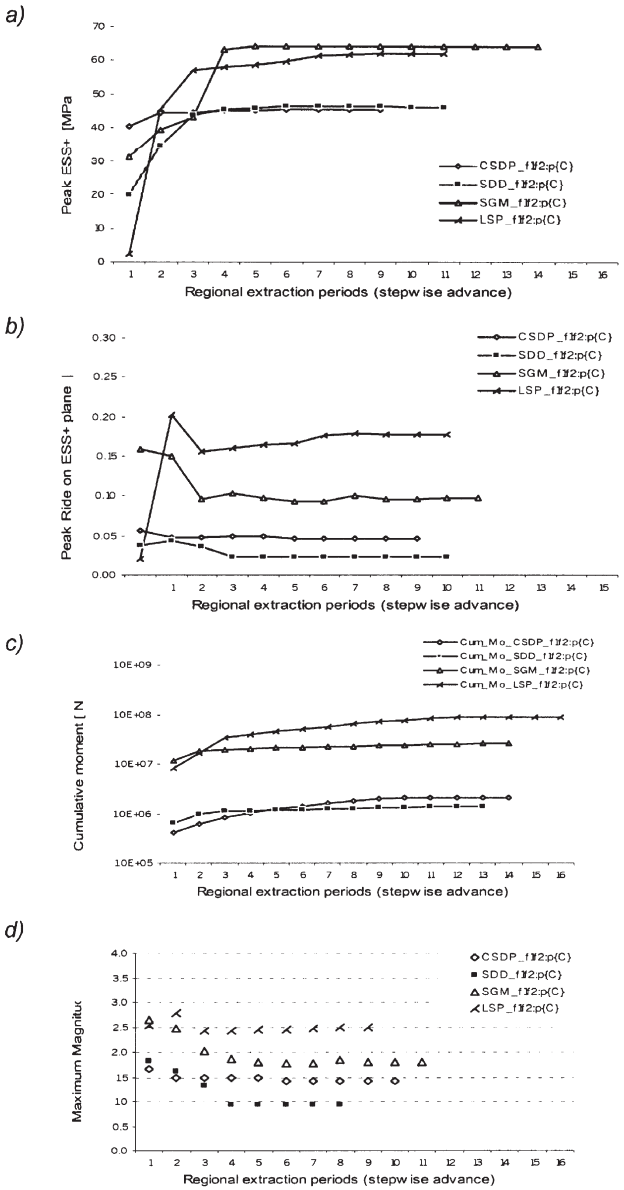

Figure 13—Stepwise comparison of parameters used to assess seismic risk of slip-type events on dyke f_1f_2:π{C} in the four layouts. a) shows the peak positive ESS, b) the peak-ride on the feature plane, c) the cumulative seismic moment and d) the inferred maximum magnitude

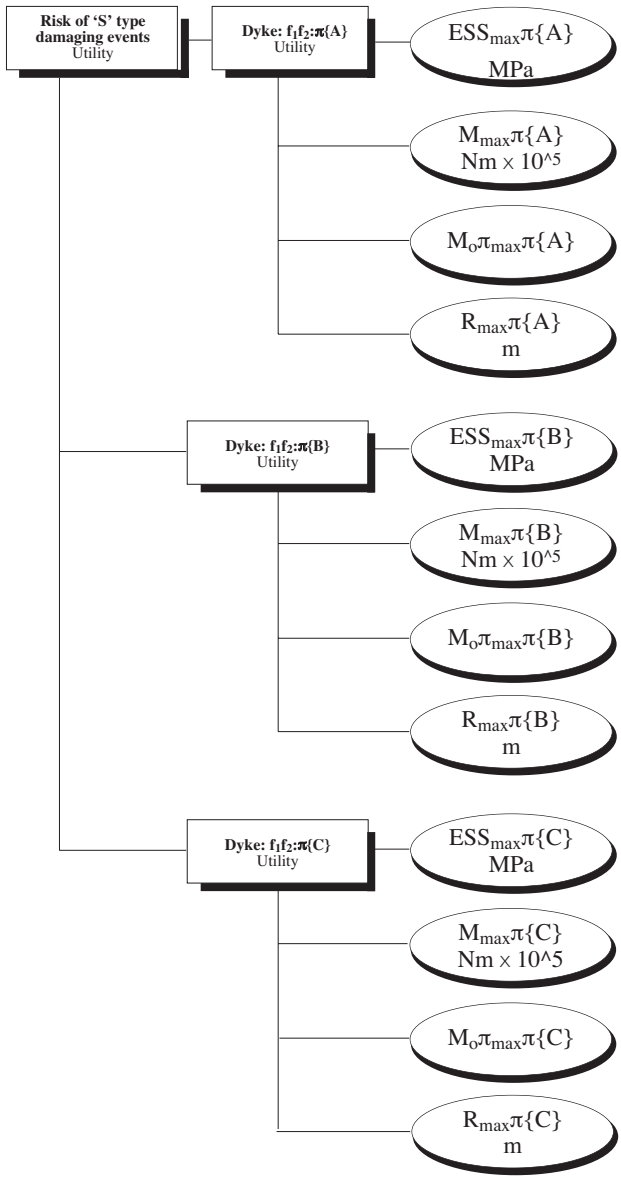

Figure 14—Utility-type model to determine overall risk of slip-events in a given layout. In this scheme, overall risk is the inverse of 'utility'. The model takes into consideration the combined effects of shear slip along three geological features existent in each layout model

Table IV

Summary results of multi-step seismic risk analysis

Feature: f^1,f^2:π{A}	M_{max}	Rank	$ESS+_{max}$	Rank	R_{max}	Rank	Mo_{max}	Rank
CSDP	4E+05	1	46	1	0.06	2	2.5	1
SDD	7E+05	2	46	2	0.04	1	2.6	2
SGM	1E+07	3	64	4	0.16	3	3.4	3
LSP	2E+07	4	62	3	0.20	4	3.6	4
Feature: f^1f^2:π{B}	M_{max}	Rank	$ESS+_{max}$	Rank	R_{max}	Rank	Mo_{max}	Rank
CSDP	5E+06	3	54	3	0.12	3	3.2	3
SDD	4E+05	1	47	1	0.04	1	2.5	1
SGM	6E+05	2	59	4	0.11	2	2.6	2
LSP	1E+07	4	53	2	0.25	4	3.4	4
Feature: f_1f_2:π{C}	M_{max}	Rank	$ESS+_{max}$	Rank	R_{max}	Rank	Mo_{max}	Rank
CSDP	5E+06	3	48	3	0.12	2	3.2	3
SDD	2E+06	1	37	1	0.08	1	2.9	1
SGM	4E+06	2	53	4	0.19	3	3.1	2
LSP	8E+07	4	40	2	0.24	4	4.0	4

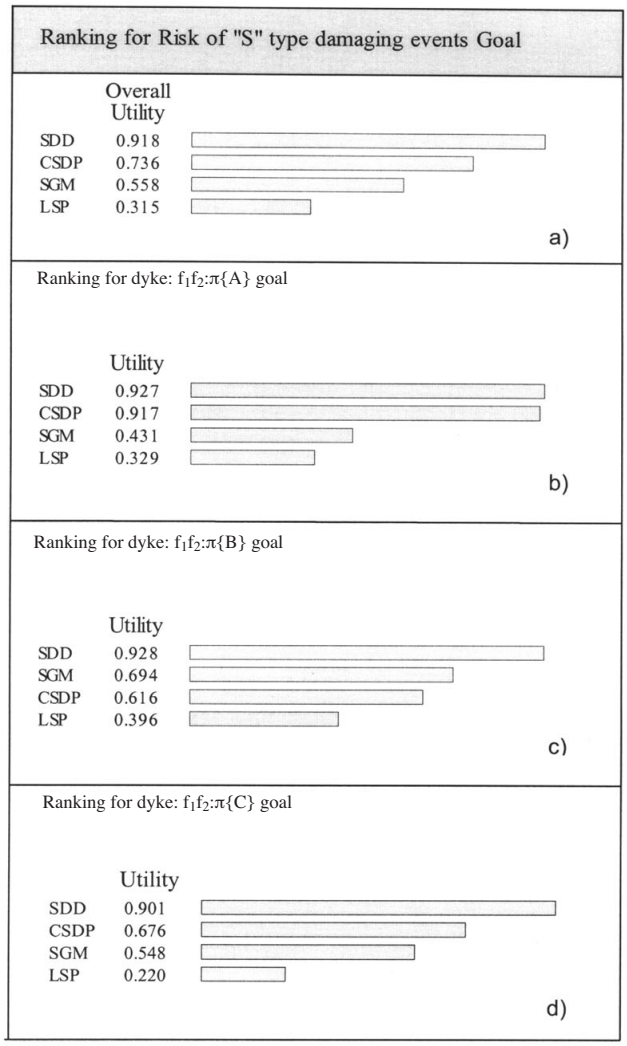

Figure 15—Ranking of layout seismic risk based on utility analysis. As applied in the current context, risk is the inverse of utility

developed, i.e. developed after stoping has advanced above. These excavations, termed follow-behind tunnels, are thus developed in stress-relieved, less confined ground. Footwall excavations in SGM, SDD and CSDP layouts are generally developed in virgin stress conditions, often in well-confined rock masses and prior to any stoping taking place in the vicinity. These tunnels do not normally require extensive support during the development stage. Subsequent rock mass changes caused by the effects of stoping will determine the support requirements thereof. Main service excavations such as haulages and return airways are developed along strike (i.e. with orientation perpendicular to that of dip-orientated pillars). The consequence of this geometry is that short sections of these tunnels pass beneath alternating zones of high and low stress (e.g. Figure 17). Haulages and RAWs are long-term excavations and, unlike replacement-haulages in LSP layouts, no provision is made for these tunnels in SGM, SDD and CSDP layouts to be replaced at any stage during the life of the mine.

RCF in footwall tunnels

(a) A typical distribution of RCF values surrounding a LSP tunnel beneath a 240 m wide longwall is shown in Figure 16. The footwall follow-behind tunnel lags behind the stope face, with the development end within a region where RCF<0.3.

(b) The SGM layout has 40 m wide dip-pillars separating 160 m wide stopes. The footwall haulages were positioned 90 m below reef. The high RCF values beneath pillars show that the rockwall conditions are likely to be poor (Figure 17). These adverse conditions were avoided in subsequent SGM designs by increasing the average middling to reef to 120 m. The degree of variation of RCFs in SGM tunnels depends on the stoping sequence. When the influence of stoping is greatest, RCF values along the tunnel peak at 1.7. Once stoping of a particular raise line is complete, RCF values along the tunnel 120 m decrease to 1.2 beneath pillars, and to 0.7 beneath the centre of the mined-out stopes.

(c) In the SDD layout the 25 m wide dip-pillars separate 75 m wide stopes, with the tunnel positioned roughly 50 m in the footwall. RCF values along all elements of SDD tunnel paths peak at 2.0. Once stoping on a particular raise line is complete, RCF values drop to 1.6 beneath pillars and to 0.7 below raise lines. Consequently, long-term support measures need be less stringent in those sections of tunnel sited beneath stopes.

(d) In the CSDP layout the 40 m dip-pillars separate 140 m wide stopes, with the tunnel positioned roughly 90 m in the footwall. The length of tunnels beneath pillars affected by high RCF values is shorter in CSDP than in the SGM

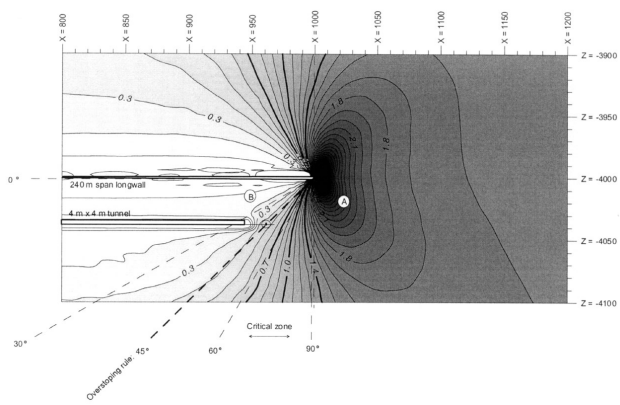

Figure 16—Cross-section along the strike direction of mining showing the distribution of RCF beneath a LSP stope. Mining occurs at an average depth of 4000 m below surface and the plan of reef dips 23°

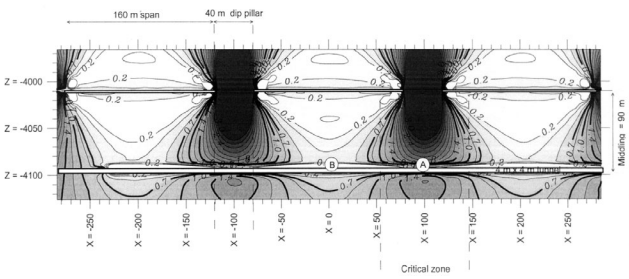

Figure 17—Cross-section along the strike direction of mining showing the distribution of RCF beneath SGM stopes in three raise lines. Mining occurs at an average depth of 4000 m below surface and the plan of reef dips 23°

layouts. RCF values peak at 1.7, but once stoping reaches completion on a particular raise line, the RCF values decrease to 1.6 beneath the pillars and to 0.6 below raise lines.

Extent of zones with poor rock conditions

Critical zones are those sections of a tunnel along which RCF >1, i.e. conditions change from 'moderate' to 'deteriorate' status. The extent of the critical zone beneath each pillar is important for arriving at adequate support measures in footwall tunnels. RCF varies harmonically along tunnels beneath SGM, SDD and CSDP layouts (see Figure 18 and Table V). SGM and CSDP designs have similar risks of seismic damage, while conditions in SDD tunnels should be somewhat better.

Probabilistic analysis of RCF

If the entire population of RCFs along footwall tunnels in all layouts is considered, a probability distribution of RCF values along the tunnel paths can be determined (see Figure 19). The probability for observing excellent to moderate conditions (RCF<1) along tunnels in LSP layouts is about 0.43, compared to 0.20 for SDD, 0.14 for SGM and 0.12 for CSDP layouts. By inference, we establish that the LSP layout design offers the best chance for limiting seismic damage along footwall strata, should an event occur.

Risk of seismic damage in tunnels as a function of depth

Three depth horizons were considered, and probability distributions similar to that in Figure 19 were determined for the stoping depths of 3000 m, 4000 m and 5000 m. The relative increase is calculated relative to 3000 m, which is assumed representative of current deep level mines. Figure 20 shows the extent of tunnel rockwall conditions designated 'deteriorate' to 'severe' increases dramatically for all layouts using pre-developed grid-type footwall infrastructure (SGM, SDD and CSDP).

Conclusions

The task of the mine designer is to ensure that mining can take place as safely and profitably as possible, thereby reducing the risk of deep-level mining to both the underground worker and the investor. However, parameters over which the designer has no control, such as rock strength and ore grade, may vary significantly. Furthermore, the designer has numerous options to consider, such as the mining layout, pillar and stope dimensions, and position of tunnels. We propose that probabilistic methods are powerful tools that will enable the designer to search for and find optimum solutions to extremely complex problems.

We have applied the probabilistic approach using conventional estimators of rockburst risk (ERR, ESS and RCF) to four layouts that are currently used to mine the deep tabular orebodies of the Witwatersrand basin. We have deliberately avoided making statements about which layout is 'best', as in each case there are opportunities to lower the rockburst risk by adjusting the mining geometry, extraction sequence or mining rules (scheduling times, etc.). For example, the mine designer could opt to stiffen the overall regional system by changing pillar dimensions and mining spans, or else introduce backfill. Unfortunately, we found that currently

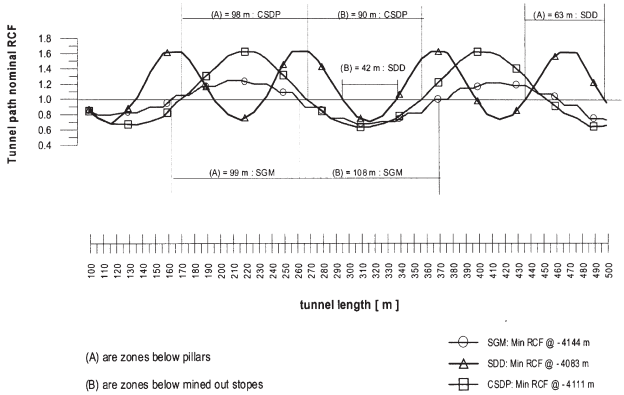

Figure 18—Sizes of zones of sustained stress peak (i.e. zones A, also termed critical zone) and zones of load suppressing (zones B) in footwall tunnels of gridtype development infrastructure

Table V

Average length of 'rockwall condition zones' along footwall tunnels of three mine layouts

	Zone (A) below pillars [deteriorate to severe]	Zone (B) below stopes [excellent to moderate]	Middling to reef	Surface elevation
SGM	99 m	108 m	120 m	4144 m
SDD	63 m	42 m	50 m	4083 m
CSDP	98 m	90 m	90 m	4111 m

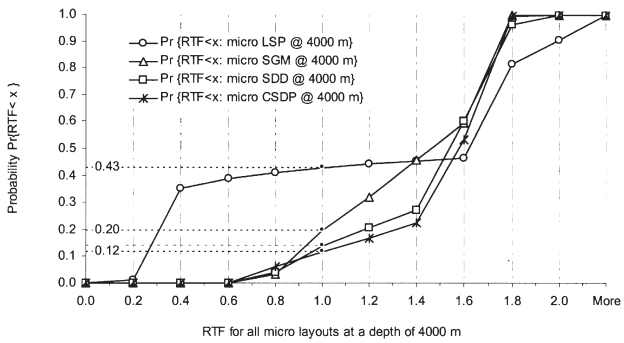

Figure 19—Cumulative probability distribution of RCF along footwall tunnels of the four layout designs

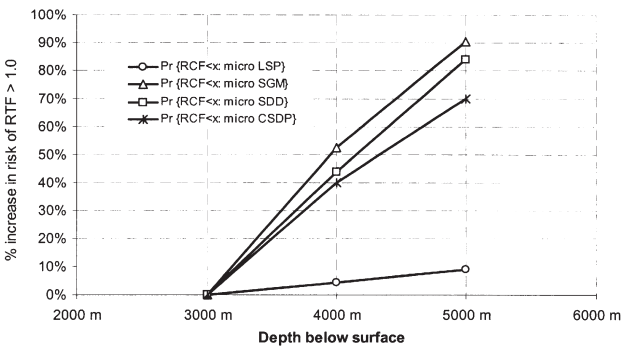

Figure 20–Relative increase in risk of 'unsupported' footwall tunnels assuming 'deteriorate' rockwall conditions for increasing depth

available rock engineering software is inadequate for the task as time consuming pre- and post-processing of models and data was required. Furthermore, there are other considerations in selecting layouts, such as the efficiency and cost of cooling, ventilation, and the transportation of men, materials and rock.

Lastly, it is not sufficient simply to identify and quantify risk and optimize mine plans. A holistic risk management strategy must also involve continuous improvement in competence, auditing of mining practice, and the monitoring of rock mass behaviour.

Acknowledgements

The sponsors of the DEEPMINE Programme are thanked for granting permission to publish this paper.

References

CSIR, 2000. MINSIM 2000 stress analysis software. Comprises applications: MinPlan, MinPrep, MinSolve; MinPost. CSIR Mining Technology. Johannesburg. South Africa.

HUDSON, J.A. and FAIRHURST, C. Tensile strength, Weibull's theory and a general statistical approach to rock failure. In: *Structure, solid mechanics and engineering design*. Proc. Southampton 1969. *Civil engineering materials conf.* (Ed. Te'eni, M.), pp. 901–914. Wiley-Interscience, London (1969).

LIGHTFOOT, N. and MACCELARI, M.J. *Numerical modelling of mine workings. Volume I*: Principles of Numerical Modelling. SIMRAC; CSIR - Mining Technology. Johannesburg, South Africa. 1999.

RYDER, J.A. Excess shear stress in the assessment of geologically hazardous situations *J. S. Afr. Inst. Min. Metall*. vol. 88, no. 1. Jan. 1988. pp. 27–39.

ROWE, W.D. *An anatomy of risk*. Wiley-Interscience Publications. John Wiley and Sons. New York, 1977. 488 pp.

SANOPOULOS, L. and ASWEGEN, G. Limited mine layout design audit for rock mass stability. ISS International Limited. Subtask Report to Task 3.2.1. Report No. DM321-REP-001. Deepmine, 5 March 2001.

SMITH, G.R. Logical Decisions®. Decision Support Software. Golden, CO, USA. 1998.

SPOTTISWOODE, S.M. Total seismicity, and the application of ESS to mining layouts, *J. S. Afr. Inst. Min. and Metall.*, vol. 88, 1988. pp. 109–116.

SPOTTISWOODE, S.M. Energy Release rate with limits to on-reef stress. *Proc. 1st Southern African Rock Engineering Symposium*, Ed. R.G. Gürtunca and T.O. Hagan, SANGORM, 1997. pp. 252–258.

SPOTTISWOODE, S.M. Modelling seismicity and creep on multiple stope-parallel layers. *Proc. 2nd Southern African Rock Engineering Symposium*, Ed. T.O. Hagan, ISRM Regional Symposium, 1999. pp. 155–159.

SPOTTISWOODE, S.M. and NXUMALO, M. Synthetic seismicity: characteristic of layout risk. Deepmine Collaborative Research Programme; Addendum to Deepmine Task 3.2.1 Final Report Project Report. (Ed.) Vieira, F.M.C.C.; Report No. 2001. pp. 2000–0169.

STORRAR, C.D. *South African Mine Valuation*. Chamber of Mines of South Africa. Johannesburg. 1981.

VAN ASWEGEN, G., SPOTTISWOODE, S.M., and NAICKER, N. The relationship between depth and seismicity. Deepmine Collaborative Research Programme; Research Task 5.1.1. ISS Intern. and CSIR Miningtek: Final Report no. DM511-REP-001-0. 2000.

VIEIRA, F.M.C.C. The evaluation of the rock engineering aspects of SMDP mining at great depth and the use of a multiple-attribute utility for mine layout assessment. *2nd Southern African Rock Engineering Symposium*, Johannesburg. 1999.

VIEIRA, F.M.C.C., DIERING, D.H., and DURRHEIM, R.J. Methods to Mine the Ultra-Deep Tabular Gold-Bearing Reefs of the Witwatersrand Basin, South Africa. In: Techniques in Underground Mining by R.L. Bullock and W. Hustrulid (editors) (in press). 2000.

WANE, M.T., HASSIALIS, M.D., and BOSHKOV, S. The probabilistic nature of failure in the geological universe. *Proc. 4th Int. Conf. Strata Control Rock Mech.*, Columbia Univ. 1964. pp. 324–329. ◆